ORIGINAL ARTICLE

Hydrodynamic connectivity and dispersal patterns of a transboundary species (*Pagellus bogaraveo*) in the Strait of Gibraltar and adjacent basins

Irene Nadal[1] | Simone Sammartino[2] | Jesús García-Lafuente[1] |
José C. Sánchez Garrido[1] | Juan Gil-Herrera[3] | Manuel Hidalgo[4] |
Pilar Hernández[5]

[1]Universidad de Málaga, Instituto de Biotecnología y Desarrollo Azul (IBYDA), Physical Oceanography Group, Málaga, Spain

[2]Instituto de Ingeniería Oceánica (IIO), Physical Oceanography Group, Universidad de Málaga, Málaga, Spain

[3]Centro Oceanográfico de Cádiz (IEO, CSIC), Cádiz, Spain

[4]Ecosystem Oceanography Group (GRECO), Centro Oceanográfico de Baleares (IEO, CSIC), Palma, Spain

[5]General Fisheries Commission for the Mediterranean, Technical Unit for Western Mediterranean, Food and Agriculture Organization of the United Nations, Málaga, Spain

Correspondence
Irene Nadal, Universidad de Málaga, Instituto de Biotecnología y Desarrollo Azul (IBYDA), Physical Oceanography Group, Málaga, Spain.
Email: irenenadal@ctima.uma.es

Abstract

The blackspot seabream (*Pagellus bogaraveo*) is a benthopelagic fish species highly appreciated by consumers and an important target of the Spanish and Moroccan fisheries in the transcontinental waters of the Strait of Gibraltar area. It is also one of the most exploited resources of the region, which has led to a situation of overexploitation and a notable drop of catches. To gain insight into the sustainability of this resource and certain patterns of the spatial adaptation of the species, a high-resolution circulation model coupled to a Lagrangian tracking module has been employed to investigate the dispersal pathways of blackspot seabream, using eggs and larvae (early-life-stages, ELS) as purely passive particles advected by currents. Several spawning scenarios consisting of different spatial (depths and sites) and temporal (tidal phase and strength) initial conditions have been analyzed to identify the most likely pathways of ELS dispersion. Eastward transport by the Atlantic Jet exiting the Strait of Gibraltar is the most influencing process in that dispersion. Regarding temporal fluctuations, fortnightly tidal modulation is the prevailing factor to determine the horizontal paths of the ELS, spring tides being the cause of the greatest scattering of propagules. Spawning depth in the Strait of Gibraltar is a critical condition, as revealed by the model sensitivity tests. Potential implications of the results of the study to improve the assessment and management of this species are discussed.

KEYWORDS
Alboran Sea, blackspot seabream, early-life-stages (ELS), hydrodynamic connectivity, pelagic larval duration (PLD), Strait of Gibraltar, transboundary stock

1 | INTRODUCTION

Oceanographic features largely control the dispersal of fish eggs and larvae and thereby the dynamic connectivity of geographically separated fish subpopulations (Cowen & Sponaugle, 2009). Such control is particularly tight in highly energetic areas influenced by tides, wind-driven currents and small-scale turbulence (Cowen et al., 2006; Sakina-Dorothée et al., 2010). Dynamic connectivity concerns to those interactions between the life cycle of the fish species in question and the physical processes that drive the dispersal of early life

stage individuals (ELS, hereinafter) at different spatial and temporal scales. Understanding the processes and scales controlling ELS dispersal and how connectivity influences the dynamics of the affected populations is a major challenge of special interest for vulnerable species (Cowen et al., 2006; Pineda et al., 2007), particularly relevant for species inhabiting across jurisdictional waters of different countries (Hidalgo et al., 2019; Palacios-Abrantes et al., 2020; Pinsky et al., 2018). Resolving the mechanisms controlling ELS dispersal entails the understanding of the relevant physical processes and how the species mediate the physical outcome (García-Lafuente, Sánchez-Garrido, et al., 2021). Currently, studies of dispersal dynamics and larval connectivity are being used to provide an approach to improve fisheries management and assessment (Fogarty & Botsford, 2007; Hidalgo et al., 2019). Focusing on fisheries health in the Strait of Gibraltar (SoG hereinafter, see Figure 1), the blackspot seabream [*Pagellus bogaraveo* (Brünnich, 1768)] is one of the most affected stocks (Gil, 2006, 2010). It is targeted by local fishermen from Spain and Morocco using a special longline gear, known as *voracera*.

Landings from this shared fishery exhibit a clear decreasing trend since 2009, which shows up a vulnerability that is raising serious concerns at local and international levels in a socioeconomic context (Báez et al., 2014). In 1998, the Spanish Government introduced technical measures to manage this fishery, and few years later, the Andalusian Regional Government developed a specific fishing plan that included a biological rest period and the limitation of the number of hooks per *voracera* (Burgos et al., 2013). Transitional measures for the management of blackspot seabream in the Alboran Sea (AS, hereinafter) were primarily set out by the General Fisheries Commission for the Mediterranean (GFCM) in 2017 (Recommendation GFCM/41/2017/2). Later on, the Recommendation GFCM/43/2019/2 establishes an adaptive multiannual management plan for its sustainable exploitation in the AS. Last GFCM stock assessment indicated that the SoG and population (geographical sub-areas, hereafter GSAs, 1 and 3; see Figure 1) is overexploited and in overexploited status and, consequently, a reduction of fishing mortality towards sustainability levels was recommended (GFCM, 2021). Even so, the sustainability of blackspot seabream fisheries requires more efforts (Gil-Herrera et al., 2021).

The optimization of the fishery stock and the curbing of the overexploitation of the resource require further studies of population dynamics and hydrodynamic and demographic connectivity, especially during larval stages. They should address the consequences of the connectivity on the production of the stocks and other characteristics at interannual time-scales. Trying to fill these gaps, the Regional Cooperation Project for Fisheries in Western Mediterranean (CopeMed) and the GFCM of the Food and Agriculture Organization (FAO) developed the EU-funded project "*Transboundary population structure of Sardine, European hake and blackspot seabream in the Alboran Sea and adjacent waters: a multidisciplinary approach*" (TRANSBORAN; CopeMed, 2017, 2019), which focused on the management of the fishery stocks of these species in the AS and adjacent waters. One of the main objectives of the project was to understand and identify the mechanisms of larval dispersal in the area, which is

crucial to determine the populations structure and to optimize the fisheries functioning (Pineda et al., 2007; Virtanen et al., 2020).

From a hydrodynamic point of view, ELS dispersal is usually investigated by means of tracking algorithms fed by hydrodynamic numerical models (e.g., Dubois et al., 2016; Rossi et al., 2014). Some studies suggest that ELS information concerning larval behavior, egg buoyancy or diel vertical cycles is critical (Fiksen et al., 2007; Sundelöf & Jonsson, 2012), whereas others show that active swimming during ELS is negligible when compared with the effect of the drifting by the ocean currents (Hidalgo et al., 2019). This biological aspect has not been elucidated yet for the blackspot seabream. Nevertheless, the high dynamics of the area strongly supports the second hypothesis. Consequently, the present study considers the ELS as passive tracers advected by the currents and investigates their dispersion and connectivity patterns using a high-resolution ($\approx$1 km) circulation model of the SoG, the spawning area of the species (Gil, 2006, 2010), and the AS. Different scenarios have been considered in order to assess the sensitivity of the resulting patterns against the initial conditions. The scenarios include diverse spawning grounds and depths in the SoG as well as distinct hydrodynamic initial conditions associated to the tidal phase and strength (spring-neap tidal cycle) of the currents at the moment of the spawning.

The paper is organized as follows: next subsections present the main traits of the biology of the blackspot seabream and of the hydrodynamic features of the area of study. Section 2 describes the numerical model and the Lagrangian approach and provides details about the experimental procedure. Section 3 reviews and discusses the results of the numerical experiments. It has been organized into seven subsections addressing different aspects of the dependency of the specific spatial and temporal initial conditions on the ELS dispersal paths and the potential implications for fishery management of the species. Section 4 includes a summary of the results and conclusions of this work.

1.1 | Life cycle of blackspot seabream

As other Sparidae species, the blackspot seabream is a sequential protandric hermaphrodite, starting as males and then changing into females at 30–35 cm length and around 4 to 6 years age (Alcaraz et al., 1987; Gil, 2006; Krug, 1994). It grows relatively slow to a maximum size of 70 cm, weight of 4 kg and about 15 years age (Gil, 2006; Krug, 1994; Sánchez, 1983). Juveniles inhabit inshore areas while adults have deeper distribution (Desbrosses, 1932). Olivier (1928) and Desbrosses (1932) report species vertical movements during the night and in certain seasons, related to daylight and spawning. However, this has not been already demonstrated for the case of the SoG population. Fish populations are potentially able to adapt to the mean horizontal transport and dispersion pattern of its ELS by influencing the vertical position of its planktonic offspring either by its spawning behavior (fish selection of spawning area and depth) or by producing eggs of certain specific gravity (Sundby & Kristiansen, 2015). The ontogeny of the species ELS is only available from aquaculture

experiments estimating a pelagic larval duration (PLD) from 40 to 60 days (Peleteiro et al., 1997).

The AS might be considered as a hatchery and nursery area of the species (Gil et al., 2001): Juveniles are mostly caught close to the shore by recreational angling fishery, following similar patterns seen in other places like the Bay of Biscay (Lorance, 2011), the Azores Islands (Pinho et al., 2014), and the Mediterranean Sea (Biagi et al., 1998). Adults, targeted by the Spain and Morocco *voracera* fishing fleets, spawn during the first quarter of the year in the SoG (Gil, 2006, 2010). Interconnected cycles of recruitment in both sides of the nearby coastal areas of the SoG followed by juveniles returning to the grounds where the fishery takes place were suggested by Gil et al. (2001).

1.2 | Relevant hydrodynamic features of the area

The SoG connects the North Atlantic Ocean and the Mediterranean Sea and is one of the most energetic spots in the world ocean. The net freshwater deficit of the Mediterranean basin drives an archetypical baroclinic exchange that involves very large currents. Lighter Atlantic water flows into the Mediterranean basin invading the AS in the form of a swift Atlantic Jet (AJ hereinafter), while denser Mediterranean water flows underneath toward the Atlantic Ocean (García-Lafuente et al., 2013). On average, each of these flows are slightly less than 1 Sv (1Sv = 10^6 m^3 s^{-1}; García-Lafuente, Sammartino, et al., 2021; Sammartino et al., 2015), but they can quadruple the values during certain moments of the tidal cycle due to the strength of the tidal currents (García-Lafuente et al., 2000). Actually, the tide-topography interaction in the area gives rise to one of the most noticeable internal tides in the world ocean (Sánchez-Garrido et al., 2011), which displaces vertically the interface between Atlantic and Mediterranean waters by more than 100 m periodically. Also,

forced barotropic flow through the SoG driven by the changing atmospheric pressure field over the Mediterranean basin modifies the baroclinic exchange by significant fractions of their average values at few-days' timescale (García-Lafuente et al., 2002).

The general circulation of the AS is determined by the mentioned AJ (see the pioneer paper by Lanoix, 1974, or the extensive review by Parrilla and Kinder, 1987, for details). The AJ sets up two anticyclonic structures: the Western and the Eastern Alboran Gyre (WAG and EAG, respectively; see sketch of Figure 1), which exhibit seasonal and shorter time-scale variability. In winter, the WAG tends to be replaced by a coastal jet attached to the African coast (Flexas et al., 2006; Vargas-Yáñez et al., 2002). Surface variability is reduced during summer, when the atmospheric forcing is less variable (Sánchez-Garrido et al., 2013). Smaller scale processes such as tidally driven relative vorticity imported from the SoG, westerly winds and occasional AJ drifts, propitiate the formation of cyclonic eddies along the northern side of the jet in the western Alboran basin (Sánchez-Garrido et al., 2013; Sarhan et al., 2000) and also in the southern coast (Mason et al., 2019). These eddies induce upward pumping of deep waters, entailing high productivity areas favorable for mesopelagic species development (Sánchez Garrido et al., 2015).

2 | NUMERICAL DATA AND METHODS

2.1 | The hydrodynamic model

The numerical model used to simulate the hydrodynamics of the studied area is based on the MITgcm code (Marshall, Adcroft, et al., 1997; Marshall, Hill, et al., 1997), which has been already used in previous studies of this particular region (Sammartino et al., 2014; Sánchez-Garrido et al., 2011, 2013). The general configuration of the model, its advection scheme, and other technical details are provided in these
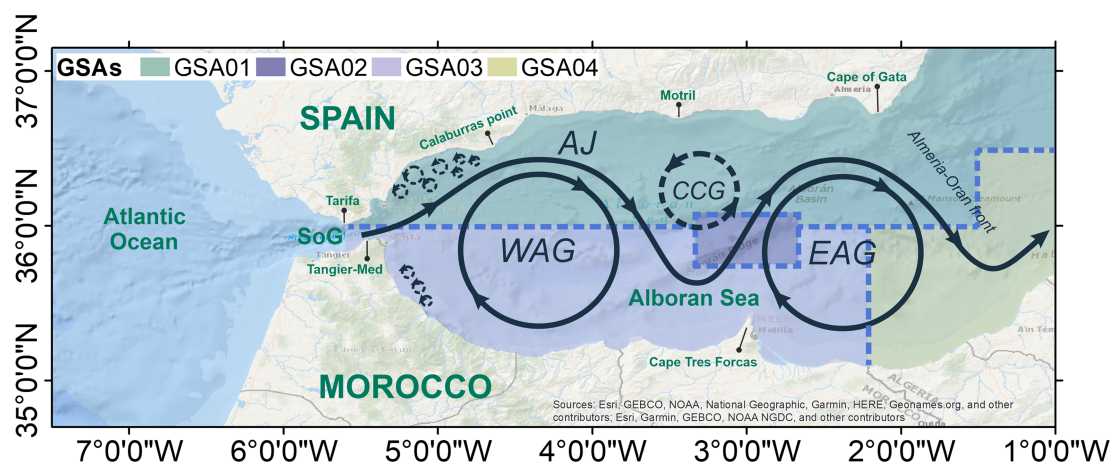

FIGURE 1 Map of the Alboran Sea showing the Strait of Gibraltar (SoG) and sketching its general surface circulation: the Atlantic Jet (AJ) and the western and eastern Alboran Gyres (WAG and EAG, respectively). CCG stands for Central Cyclonic Gyre, a weaker structure that normally develops whenever the WAG and EAG are fully developed (adapted from Sánchez-Garrido et al., 2013). Smaller cyclonic eddies, represented by dashed lines, are often found rightwards and leftwards of the AJ main path. Some relevant locations are displayed and the GSAs (1–4), defined by the GFCM (2021) are patched

works. It has been implemented on a curvilinear grid that covers the Gulf of Cadiz (from 9.4°W) and the AS to its eastern limit (around 1.6°E). The horizontal resolution and vertical discretization are uneven, being maximal in the SoG area and near the surface in the vertical (see Figure S1). At the two open lateral boundaries, the model is forced with baroclinic horizontal velocities, temperature, and salinity fields imported from CMEMS-IBI model (Sotillo et al., 2015). Tides are also prescribed in these open boundaries using the harmonic constants of the eight most important tidal constituents (the main semidiurnal: M_2, S_2, N_2, K_2, and diurnal: K_1, O_1, Q_1, P_1). The meteorologically driven barotropic flow prescribed at the SoG by the NIVMAR storm surge model (Álvarez Fanjul et al., 2001) is distributed throughout these boundaries to incorporate the meteorological forcing into the model. At surface, the model is forced with atmospheric conditions provided by the MED-Cordex model (Ruti et al., 2016). The model has been run from November 2004 to April 2005 in order to cover the most active spawning months of the blackspot seabream (Gil, 2006, 2010), and the 3D velocity field has been stored every 30 min.

In the vicinity of the SoG, but yet inside the AS, the highest variability of the velocity field is associated with the tidal dynamics of the Strait (García-Lafuente et al., 2000). Figure 2 shows the surface velocity and the kinetic energy per unit of mass (computed as $K_E = \frac{1}{2} \cdot \left(U^2 + V^2 \right)$, U and V the zonal and meridional surface velocity components, respectively) over two different periods. The panel on the left corresponds to neap tide and illustrates a surface pattern with diminished velocities. Right panel is for spring tide and presents the characteristic average circulation that uses to prevail: the AJ flowing into the AS, the WAG and EAG, a small CCG in between, and the Almeria-Oran (AO) front in the eastern limit of the AS. Both panels show similar circulation patterns, although velocity field is noticeably larger during spring than in neap tides. In fact, spring tides not only generate stronger currents and inject more energy, but also induce higher variability and, expectedly, rates of dispersion all over the

basin. Even though the simulated period does not cover a seasonal cycle, some hints of seasonal variability are reflected in the monthly averaged velocity at the surface and the sea surface height (SSH) during the simulation months (Figure S2).

2.2 | Releasing boxes and landing areas selection

To investigate the dispersion of blackspot seabream ELS in the area, a set of numerical experiments have been run and their outputs subsequently analyzed. All of them make use of what has been named "releasing boxes" and "landing areas" in this study. Releasing boxes embrace the most probable spawning areas of blackspot seabream. Three boxes have been established, two along the north and south shores of the SoG, labeled Tarifa and Tangier-Med, respectively (see inset in Figure 3), and a third one in between occupying the center-west area of the SoG (Tangier box). The three boxes not only cover what is currently thought to be the main spawning grounds of the species (Gil et al., 2001) but also address the geographical differentiation of the spawning area, which will have consequences on the spreading of the ELSs of blackspot seabream.

These spawning products are then transported by the currents and their fate is interpreted in terms of concentration within landing areas, which are understood as potential coastal nursery grounds. In a broad sense, a strip few kilometer wide along the coasts of the whole region should be considered as such. However, the remarkable spatial variability of the hydrodynamics of the region recommends the splitting of the strip into more reduced landing areas. The presence of notable topographic features such as Cape Tres Forcas, or Calaburras Point or Cape of Gata (see Figure 1) also favors this division. On the other hand, the zonal orientation of the AS suggests a mirror-like correspondence of landing areas in the north and south shores. According to these premises, a total of ten areas have been defined,
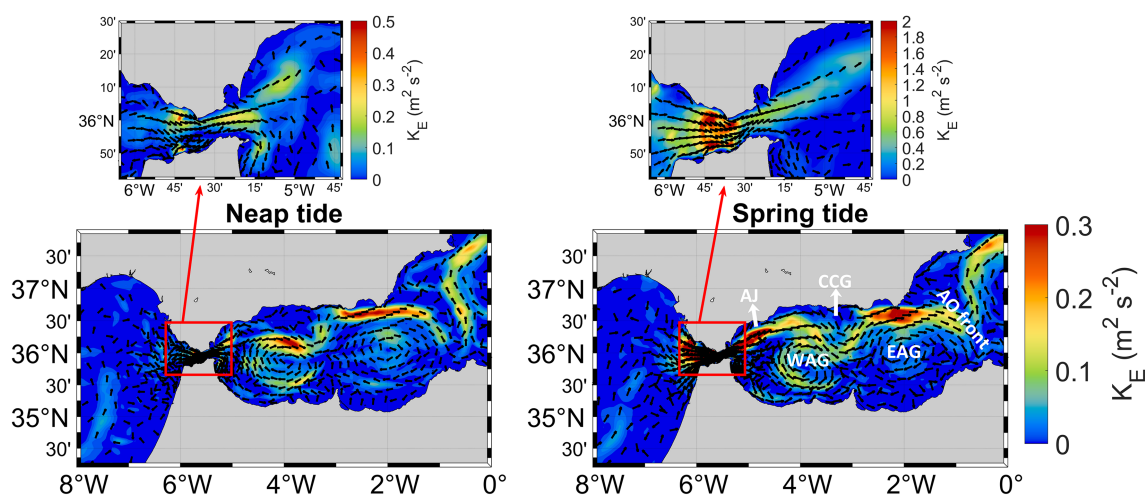

FIGURE 2 Surface current direction and kinetic energy per unit of mass (m²·s⁻²) in the AS (lower panels) and in the SoG region (upper panels) during neap (left side) and spring tide (right side). The main surface structures sketched in Figure 1 have been tagged in the lower right panel using the same acronyms
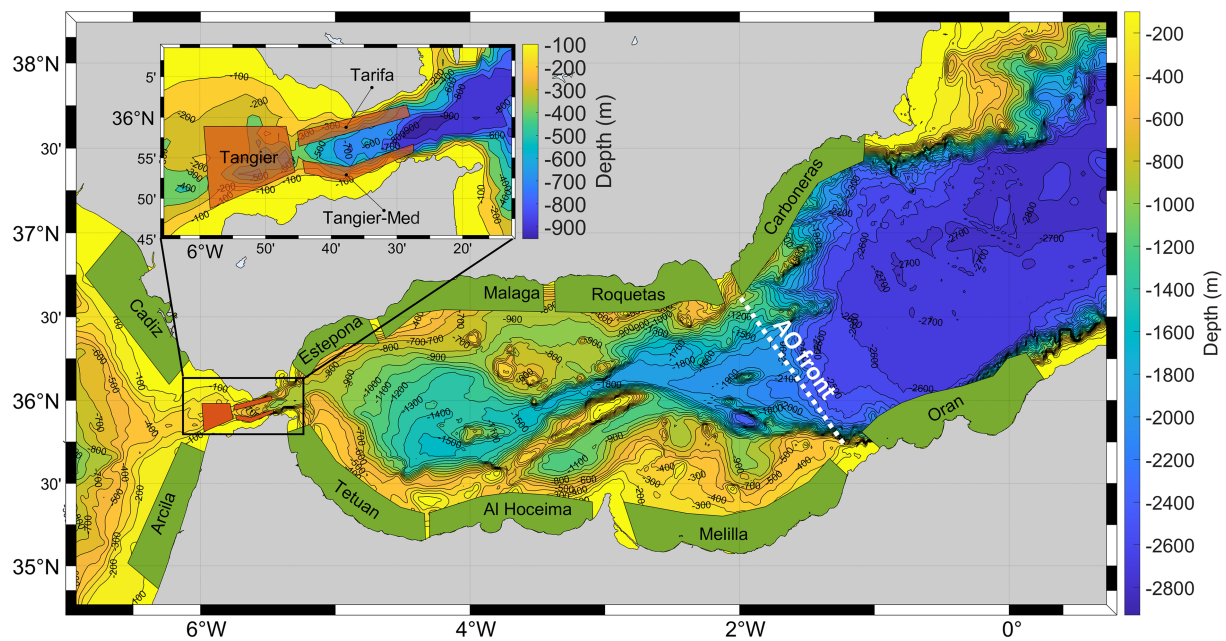
FIGURE 3 Map of the study area showing the releasing boxes of Tarifa, Tangier and Tangier-Med (brown polygons in the inset) and the landing areas of Cadiz, Estepona, Malaga, Roquetas, Carboneras, Oran, Melilla, Al Hoceima, Tetuan, and Arcila (green polygons). Adapted from CopeMed (2019)

five in each shore (Figure 3). Two of them are in the Gulf of Cadiz (Cadiz and Arcila) to check eventual westward transport of ELS, and other two in the opposite end of the region to the east of the AO front, out of the AS (Carboneras and Oran). The remaining six are located in the AS, two in the vicinity of the SoG (Estepona, Tetuan), which leaves them exposed to high-energy dynamics, two (Malaga, Al Hoceima) in the western Alboran basin under the influence of the WAG and the last two (Roquetas, Melilla) in the eastern basin under the influence of the EAG. All the landing areas are attached to the shore and subjected to different oceanographic regimes.

2.3 | Lagrangian particle tracking algorithm and experiments setup

A Lagrangian particle tracking algorithm (LaCasce, 2008; Nicolle et al., 2013, 2017) has been used to study the transport and dispersion of blackspot seabream ELS. A detailed description of the procedure can be consulted in Sammartino et al. (2018). In this Lagrangian approach, eggs and larvae are virtual passive tracers during the PLD phase. Larvae swimming capability, although barely known, appears to be insufficient to overcome the strong currents of this region and has not been considered. Therefore, ELSs are just advected by the model horizontal velocity. The horizontal trajectories have been computed by integrating the bilinearly interpolated horizontal velocity field at every grid point of the domain using a Runge–Kutta fourth-order scheme (Rossi et al., 2014). Vertical larvae migration is a sensitive information that is not yet demonstrated for the studied species, so it has been neglected for simplicity (Rodríguez et al., 2001).

In order to investigate the influence of the depth on the dispersion patterns, five different vertical spawning layers have been selected: surface (from 0 to 3 m), 12 m (from 10 to 14 m), 25 m (from 23 to 28 m), 52 m (from 48 to 56 m), and 81 m (from 76 to 87 m). To account for the effects of the time variability associated with tides, releasing times have been selected with the aim of covering a wide variety of tidal conditions that combine semidiurnal phase during four fortnightly cycles. This approach allows for replicating four times every tidal condition. Figure 4 gives information on the tidal conditions at the moment of the release for all the experiments. Lagrangian particle tracking simulations have then been run starting from every releasing time during a period of 60 days, which is the maximum PLD estimated for the blackspot seabream (Peleteiro et al., 1997).

2.4 | Pool of experiments and connectivity computation

The combination of spatial and temporal conditions gives a total of 160 numerical runs per releasing box (4 tidal phase × 2 tidal strength × 4 replicas × 5 depths), or a grand total of 480 experiments for the three boxes. The following table (Table 1) summarizes the set of numerical batches combination that has been performed with the numerical model.

As the analysis searches for ELS within each of the 10 landing areas in each experiment, a total of 4800 cases have been handled for the main analysis (to which 320 more from the depth-sensitivity study must be added). For each experiment, ∼1000 particles have been released, and the position of each particle has been computed every
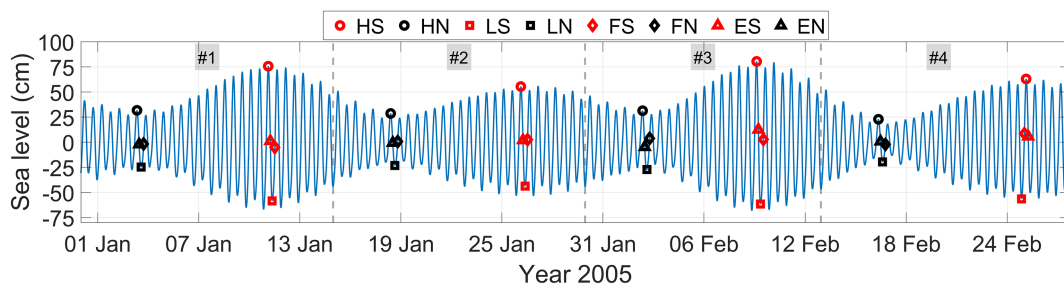
FIGURE 4 Sea level in Tarifa (blue line) during the period used for ELS release. Releasing times are shown by symbols whose meaning is indicated in the legend. It makes use of the following code to specify tidal conditions: first letter refers to tidal phase according to: H, high water; L, low water; F, maximum flood (westward) tidal current; E, maximum ebb (eastward) tidal current. Second letter specifies the fortnightly cycle according to: S, spring; N, neap tides. The gray vertical lines divide the series into four pieces that correspond to each replica

TABLE 1 Summary of the different spatial and temporal conditions configured in each numerical experiment

Releasing area	Spawning depth	Tidal phase	Tidal strength	Releasing times	Total
Tarifa	[1,12,25,52,81]	[High, Low, Ebb, Flood]	[Spring, Neap]	[#1, #2, #3, #4]	160
	[120,150]	[Flood, Ebb]	[Spring, Neap]	[#2, #4]	16
Tangier-Med	[1,12,25,52,81]	[High, Low, Ebb, Flood]	[Spring, Neap]	[#1, #2, #3, #4]	160
	[120,150]	[Flood, Ebb]	[Spring, Neap]	[#2, #4]	16
Tangier	[1,12,25,52,81]	[High, Low, Ebb, Flood]	[Spring, Neap]	[#1, #2, #3, #4]	160
Total					512

Note: From left to right: Releasing area refers to the assumed spawning zones of blackspot seabream. Spawning depth represent the depth of the spawning layers; the five depths in the range [1–81]m corresponds to the main analysis (black text), and depths 120 m and 150 m, to the tests carried out in the boxes of Tarifa and Tangier-Med to assess depth sensitivity (gray text; see Section 2.2 for details). Tidal phase refers to tidal conditions within the semidiurnal cycle (see also Figure 4): High and low correspond to high and low water, ebb is the time of maximum eastward tidal current, which happens mid-time from high-to-low water and flood is the time of maximum westward tidal flow (from low to high water). Tidal strength denotes spring and neap tides within the fortnightly cycle. Releasing times refer to the four replicas of every single experiment carried out in different times, as indicated by the numbered boxes in Figure 4. Last column is the total batch of experiments for the main analyses and the sensitivity tests.

FIGURE 5 Time series of the percentage of ELS released in Tarifa box at the surface that were found in Estepona landing area as a function of time, in a high-spring (HS) tide scenario. Red dot indicates the maximum value of 94.85% on day 7
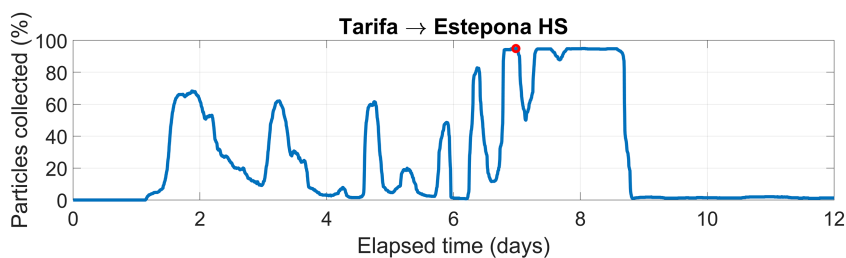
5 min. The huge amount of information needs to be processed and summarized in order to depict a relatively straightforward pattern of the ELS dispersal pathways. From an ecological point of view, dynamic connectivity is usually assessed as the percentage of particles (ELS) collected in a landing area b at a time t ($p_b(t)$) compared with those released in box a (p_a) (Cowen et al., 2006; Crochelet et al., 2016; Nicolle et al., 2017; Gamoyo et al., 2019), where t corresponds to a certain PLD, or to a fraction of it, which is fixed *a-priori*:

$$C_{a \to b}(t) = \frac{p_b(t)}{p_a} \cdot 100$$

In these works, the output usually consists of a connectivity squared matrix in which each cell is the probability of exchange of individuals between regions (row and column of the matrix), and the diagonal stands for the self-recruitment, that is, the percentage of ELS released and settled in the same box (Cowen et al., 2006). However, this approach is inappropriate in this study for two reasons. First, releasing boxes are different from landing areas because of the biological habits of the blackspot seabream, which has its only spawning area in the SoG. Hence, a reciprocal connectivity matrix is not feasible. Second, the strong and highly variable dynamics of the region makes the propagules to be swiftly advected away shortly after the release, hampering self-recruitment (Gil, 2006, 2010).

Figure 5 illustrates the shortcomings of this standard approach when it is applied to this study. It shows the time evolution during the first 12 days of simulation of the percentage of particles collected in Estepona landing area that were released at the surface in Tarifa releasing box (see Figure 3) under high-spring tidal conditions. The percentage may change from 10% to 90% in few hours (also the reciprocal), which makes meaningless the computation of the connectivity at a given time because of its strong dependence on the selected instant: the resulting value will not be representative.

In order to cope with this limitation, an alternative connectivity definition is adopted as the maximum percentage of particles (MPoP hereinafter) collected in each landing area throughout the total duration of simulation (60 days; see Section 2.3):

$$C_{a \to b} = \max\left(\frac{p_b(t)}{p_a}\right) \cdot 100.$$

Associated with this maximum percentage is the time at which it is achieved (time of maximum connectivity; ToMC hereinafter). This time is of concern as far as it must be compared with the actual PLD. Notice that contrary to the fixed time interval, the ToMC is not imposed or prescribed *a-priori*, but it is deduced from the analysis.

3 | RESULTS AND DISCUSSION

3.1 | MPoP and ToMC averages

Table 2 shows the MPoP released at the three boxes that were found in the different landing areas and the ToMC when this percentage is attained. They are averaged over the whole combination of spatial and temporal releasing conditions and provide global connectivity values that summarize the huge amount of information generated in the study. Table 2 highlights the fundamental role of the eastward flowing AJ, which is responsible for the direct spread of the ELS released in the SoG toward the AS and the nearly null abundance of particles in the Atlantic landing areas of Cadiz and Arcila.

A high connectivity (i.e., high value of MPoP) for Tarifa releasing box is observed in Malaga, Estepona, and Roquetas landing areas (45%, 38%, and 17%, respectively), followed by Oran (14%). This spatial pattern is to be expected as the AJ acts as the main advection mechanism (see Figure 1). Carboneras landing area, located outside of the AS on the northern shore, stands apart from the path of this stream and, consequently, the MPoP falls well below the previous values. A weak north-to-south connectivity is inferred from the non-null MPoP of 8% computed in Tetuan and Al Hoceima. This spatial distribution is consistent with results of larvae distribution obtained from samples collected during a scientific survey carried out in the area in the late winter 2020: a considerable number of larvae (∼8 mm length) of *P. bogaraveo* were collected in the AS, the greatest abundance (from 10 to 14.96 larvae 10 m^{-2}) having been found in Estepona and Malaga coasts (TRANSBORAN survey; J.M. Rodríguez, Pers. Comm.).

Similar zonal spread is found in the case of Tangier-Med releasing box, the southern counterpart of Tarifa box. Highest connectivity is reached in Tetuan and Al Hoceima in the south shore (MPoP of 45% and 17%, respectively). Again, a south-to-north connection is suggested by the significant MPoP of 11% and 8% in Malaga and Estepona, respectively, though the associated standard deviation, which is comparable to the mean, sheds uncertainty on the result. Roquetas and Oran areas have values of 5%, compatible with the isolation effect of the eastern rim of the WAG and the own EAG. This effect would also explain the very low values in Melilla and Carboneras (4% and 2%, respectively). Results for Tangier releasing box are similar to those of Tangier-Med. The reason is the Coriolis force that deflects particles to the south within the limits of the very SoG before the AJ

TABLE 2 Maximum percentage of particles (MPoP column) and time of maximum connectivity (ToMC column) of ELS with their corresponding standard deviations for all landing areas and releasing boxes, averaged for all scenarios of initial conditions

Landing area		Tarifa		Tangier-Med		Tangier	
		MPoP (%)	ToMC (days)	MPoP (%)	ToMC (days)	MPoP (%)	ToMC (days)
Northern coast	Cadiz	0 ± 0*	1 ± 3	0	-	0 ± 0*	1 ± 4
	Estepona	38 ± 11	4 ± 3	8 ± 8	21 ± 9	10 ± 6	13 ± 6
	Malaga	45 ± 12	7 ± 3	11 ± 8	22 ± 9	15 ± 7	11 ± 6
	Roquetas	17 ± 8	22 ± 8	5 ± 4	32 ± 6	5 ± 4	26 ± 7
	Carboneras	6 ± 4	31 ± 7	2 ± 3	33 ± 6	2 ± 2	35 ± 6
Southern coast	Arcila	0	-	0 ± 0*	1 ± 2	1 ± 2	5 ± 5
	Tetuan	8 ± 5	30 ± 13	45 ± 19	25 ± 9	33 ± 17	25 ± 7
	Al Hoceima	8 ± 5	34 ± 8	17 ± 18	40 ± 9	14 ± 13	41 ± 11
	Melilla	6 ± 3	41 ± 10	4 ± 3	46 ± 8	3 ± 2	47 ± 9
	Oran	14 ± 4	36 ± 7	5 ± 3	42 ± 6	6 ± 4	38 ± 8

Note: Landing areas have been grouped according to its geographical location. Asterisks indicate values of MPoP very close to zero (that round to cero), but not strictly null. In such situation, the ToMC is meaningless, and these cases are ignored and not discussed in the text. The two special cases of Tarifa–Arcila and Tangier-Med–Cadiz in which MPoP is strictly null; the ToMC is not defined.

spreads into the AS (Albérola et al., 1995). Therefore, once the ELSs enter the AS, their trajectories should not be much different regardless the particles were released in one box or the other.

ToMCs in Table 2 are consistent with the ELS dispersal inferred from the MPoP analysis. Shorter ToMCs are found in the landing areas closer to the releasing boxes. For particles released in Tarifa box, the shortest time is found in Estepona area (4 days). The result applies for Tangier-Med and Tangier boxes and Tetuan landing area in the southern coast (3 and 4 days, respectively). A shorter ToMC is obtained for Tangier box and Arcila area (1 day), but the very low MPoP of 1% in the area makes it not worth discussing. As distances increase, ToMC also does. In the case of Tarifa box and for northern landing areas, the greatest ToMC is found in Carboneras, the easternmost area (31 days). The same applies in the south coast, where the easternmost area (Oran) shows ToMC of 46 and 47 days with Tangier-Med and Tangier boxes, respectively. A curious case that deserves comment is that the northern landing areas have shorter ToMC with these two releasing boxes than the areas in the south (except for Tetuan). The interpretation of this somewhat anti-intuitive result is the advection of ELS by the western rim of the WAG towards the north shore. Once there, the products follow similar trajectories as the particles released in Tarifa box.

These scenario-averaged values reflect the prevailing role of the main dynamic structures of the SoG-AS system on the ELS dispersion and provide foreseeable connectivity patterns. Nonetheless, the large standard deviations (uncertainties) associated to the mean values reveal high variability related to the temporal and spatial variability of the SoG hydrodynamics as well as to the very location of the releasing boxes. These issues are addressed next for Tarifa (Section 3.2.1) and Tangier-Med (Section 3.2.2) boxes. Tangier box is presented in Figure S3 due to the aforementioned similitude with Tangier-Med, and it is not discussed here.

3.2 | Release area dependency

3.2.1 | Tarifa releasing box

Table 2 shows that, as a result of the advection by the AJ, the main connections of ELS released at the surface in Tarifa box take place with the northwestern areas of the AS. However, some differences appear when specific tidal conditions and depths are considered (Figure 6). Figure 6a shows that the highest connectivity in Estepona for surface release is achieved under ebb (E) condition in spring (S) tide (~60%), when the eastward flow in the SoG is boosted by the strong ebb current of spring tides. The same applies for near-surface releases, 12 and 25 m, which give MPoP values of ~63% and ~61%, respectively. In Malaga, MPoP is consistently greater and, somewhat paradoxically, ToMC is smaller in neap than in spring tides (Figure 6b). The behavior is reproduced by the remaining landing areas of the northern coast. As the distance of the landing area increases, however, the ratio of MPoP neap/spring increases until it reaches the highest value in the farthest landing area of Carboneras (Figure 6a).

The effect that initial conditions in Tarifa box has on the dispersal patterns is less defined in the southern landing areas. MPoPs are systematically inferior to their mirror area in the northern shore except for the two easternmost areas, with Oran showing a slightly higher MPoP than Carboneras. Such structure emphasizes the fact that north-to-south connectivity is less achievable than west-to-east connectivity due to the role of hydrodynamic barrier played by the AJ for meridional exchange. ToMCs are consequently greater than in the northern areas, except for Tetuan in spring tides, where they are similar to those found in Estepona in the north (Figure 6b).

The behavior in Tetuan contrasts with the much larger ToMCs in the other southern landing areas, which are rather independent of the tidal variability. Two different mechanisms seem to be at work. Particle scattering promoted by the intensified inflow would be the reason for the reduced ToMC in Tetuan during spring tides (Figure 6b) and for the relatively large MPoP of 23% under FS conditions in particular (Figure 6a). ToMCs in the three other areas, on the contrary, are rather independent of tidal conditions (Figure 6b). The interpretation given to this different response is that Tetuan area is directly reachable by southeastward trajectories scattered from Tarifa releasing box during the spring tide periods of enhanced currents. This process is unfeasible for the three other areas where particles will most likely arrive after completing one WAG turn around at least. It requires a time long enough to smooth out the effects of the SoG tide and the particles end up being transported by a tidal-free large-scale circulation that propitiates ToMC as large as 40 days in Al Hoceima, in sharp contrast with the scarce 6 days of Tetuan in spring tides (Figure 6b).

3.2.2 | Tangier-Med releasing box

The most obvious feature is the high MPoP in the nearest eastward landing area of Tetuan, increased during spring tides to values of ~60% (Figure 7a). The behavior resembles the east-to-west connectivity between Tarifa and Estepona area in the northern shore. Both would have the same cause, which is the zonal advection by the AJ. But the similitude Tarifa-northern areas *versus* Tangier-Med-southern areas finishes just here. Whereas in the first case MPoPs were clearly higher in all northern areas of the AS, in the case of Tangier-Med releasing box, south areas of Al Hoceima and Melilla have MPoP of the same magnitude, if not less, than in the north areas. In other words, zonal connectivity in the south is not as efficient as in the north, except for Tetuan area.

The explanation provided for this unexpected behavior is that the coastal eddy that usually forms south of the AJ and close to the African shore at the exit of the SoG (Sánchez-Garrido et al., 2013; see Figures 1 and 2) favors high MPoPs in the Tetuan area. This structure propitiates ELS retention. The trapped propagules can be eventually transferred to the western rim of the WAG and advected to the northern coast, making south-to-north connectivity feasible, and hampering west-to-east transport. The rather low values of MPoP in the upper layers of the northern areas indicate that the connection is weak. However, and this is an intriguing question, the connectivity
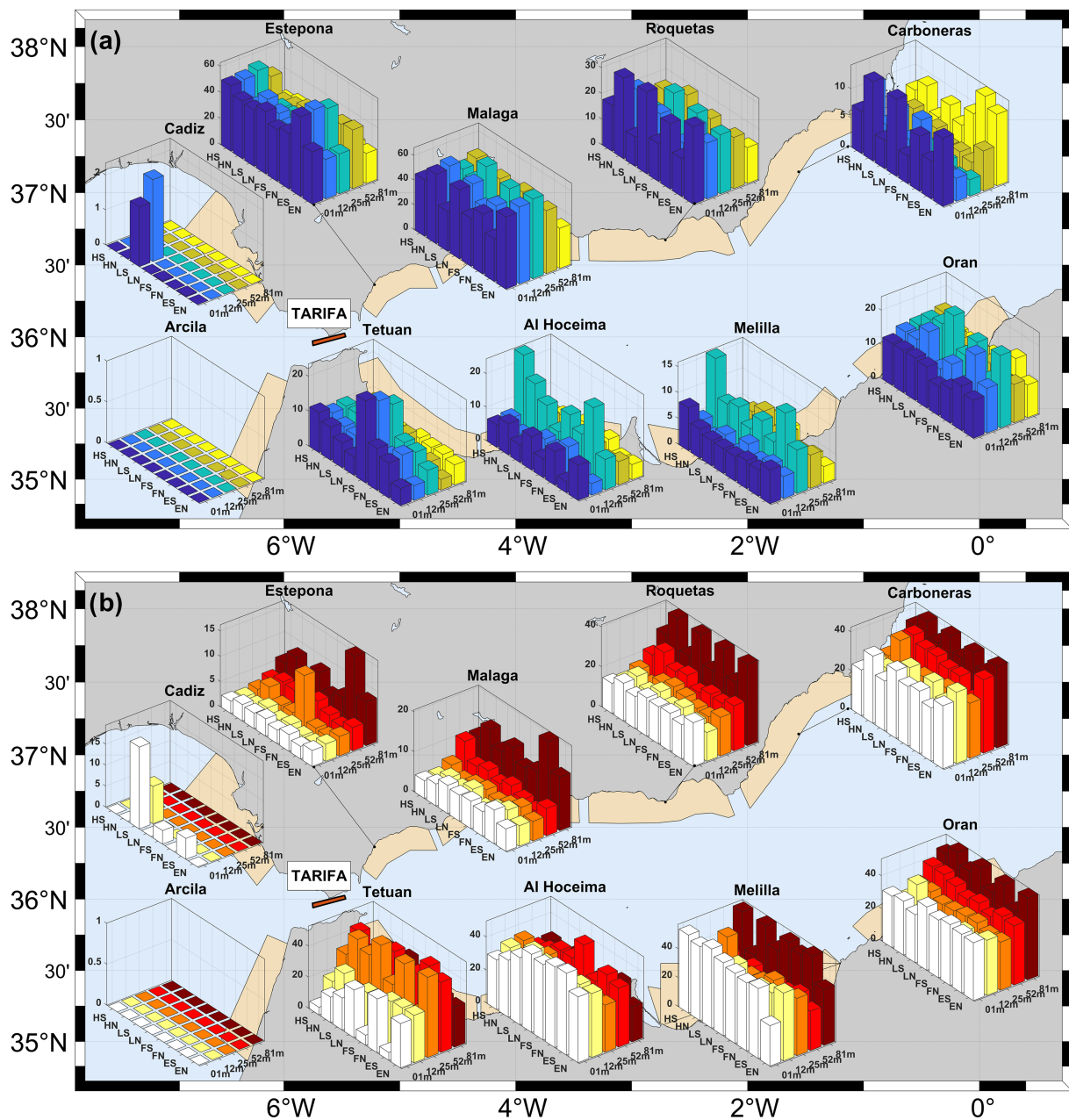
FIGURE 6 (a) Diagrams of MPoP (%) in each landing area, averaged over the four replicas of the ELS released at Tarifa box (red rectangle) for the 40 combinations of spatial (5 depths, Y-axis) and temporal (8 tidal conditions, X-axis; see acronym code in Figure 4) conditions. (b) Same as panel (a) for ToMC (days). Notice the changing Z-axis scale in the different diagrams of both panels

increases with depth (Figure 7a, yellow bars), a behavior not shared so clearly by the southern areas. Such increase raises new questions because, intuitively, connectivity should be greater at the surface, where the WAG and EAG hold stronger currents. But high velocities also entail more instabilities and turbulence that increase ELS scattering toward the interior of the Alboran basin. Velocity reduction with depth would diminish the scattering and improve the chances for ELS to arrive to farther landing areas. Consistent with this conceptual model is the fact that MPoPs at 81 m depth tend to reach absolute maxima during neap tides in Estepona area (Figure 7a).

ToMC also shows unexpected behavior. The most striking one is the large values in Tetuan area considering its proximity to the releasing box. ToMCs are even noticeably larger than those obtained for the Tarifa releasing box, particularly during spring tides (compare Figures 6b and 7b). Particles released in Tarifa box reach Tetuan area much faster than those released in Tangier-Med under the same initial conditions. It is particularly true during spring tides. But the number of particles that reaches the area is appreciably less when they come from Tarifa box (Figure 6a,b). Same conclusions apply to the other areas, the northern ones showing less ToMC than the southern ones systematically. This would confirm the aforementioned slightly better connectivity that this releasing box establishes with the north part of the AS.

Regarding the areas in the Gulf of Cadiz, Figures 6 and 7 show very poor connectivity for both releasing boxes that only occurs in
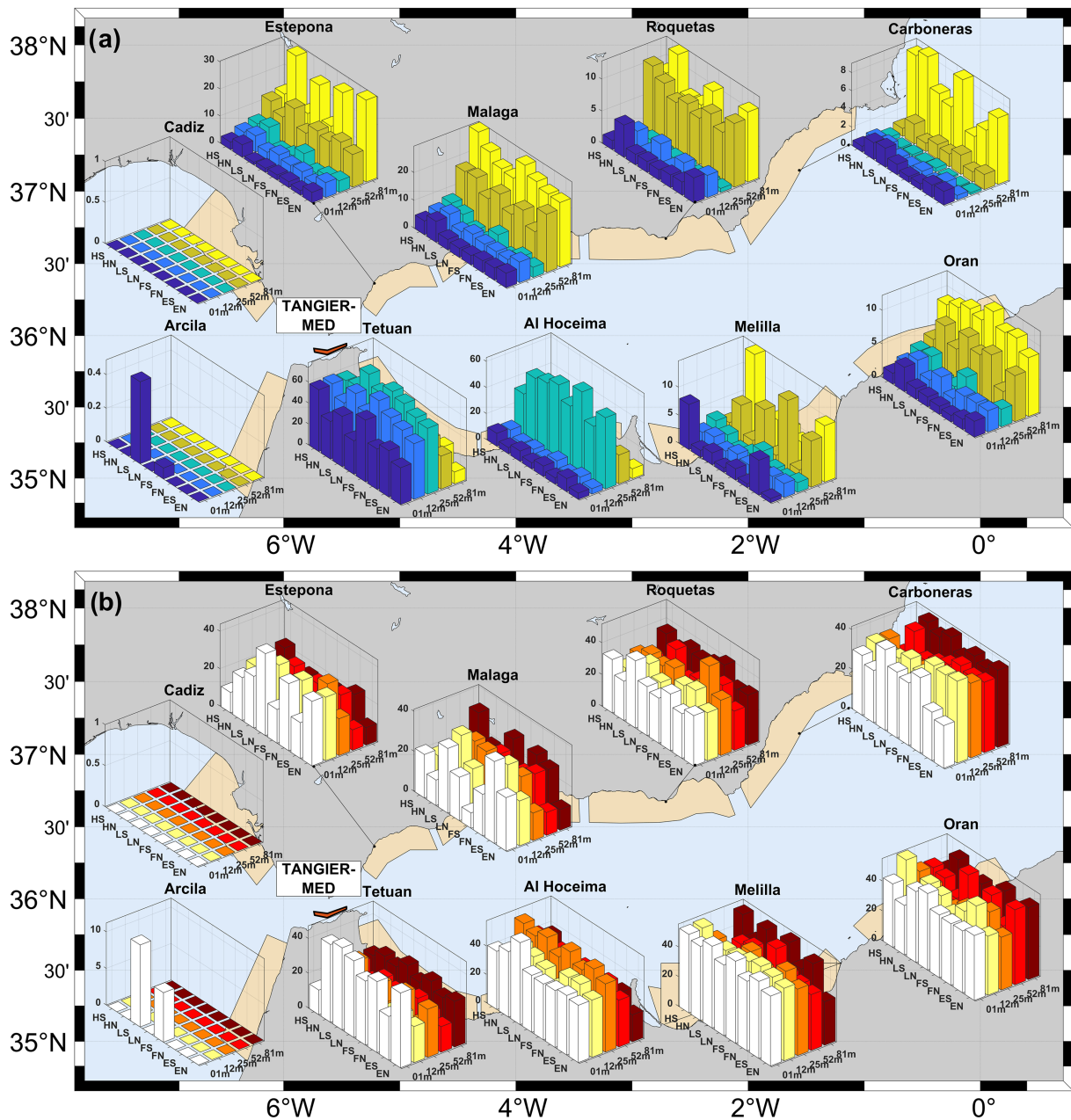
FIGURE 7 Same as Figure 6 for Tangier-Med releasing box, indicated by the red polygon

zonal direction (Tarifa-Cadiz, Tangier-Med-Arcila), not north-to-south (Tarifa-Arcila, Tangier-Med-Cadiz). It is almost uniquely met under LS initial conditions, that is, particles released at low water in spring tides. They are the most favorable conditions, as low water is the moment when barotropic tidal current reverses towards the Atlantic and spring tide enhances its intensity. The low-to-high semicycle that follows maintain relatively favorable conditions for westward transport, which causes the very low, though not null, MPoP found in those areas.

Previous discussion indicates that the dispersal of ELS is highly sensitive to the tidal phase and depth. Tidal phase and, more specifically, tidal strength related to the fortnightly spring-neap cycle is relevant for Tarifa releasing box (Figure 6) while spawning depth causes higher variability in the Tangier-Med case (Figure 7). Both initial

conditions are examined in more detail for selected cases of study in the following sections.

3.3 | Tide dependence: A case of study in the northern shore

In addition to the tidal variability that can be inferred from the abundant information in the diagrams of Figures 6 and 7, part of which has been already commented, this section addresses an illustrative case of study to assess the tidal influence. The specific instant of spawning in a given semidiurnal cycle (tidal phase) affects the initial ELS dispersion trajectories at the very beginning of the experiment, as it depends on

the direction of the instantaneous velocity at that time. Its importance, however, fades out shortly after because of its short time scale that implies reduced Lagrangian correlation scales (Taylor, 1922), leaving only the effect of the spring-neap intensity. It mostly determines the final evolution of ELS dispersion in the middle-long term, as it is demonstrated in the following case of study that involves Tarifa box and Estepona and Malaga landing areas in the north coast.

Figure 8 shows that the dispersion of ELSs released in Tarifa that induces the AJ in spring tide is greater than in neap tide (see inset) because of stronger tidal currents. When ELSs enter the AS in spring tide, the augmented scattering allows particles to reach the nearer landing areas directly, whereas particles follow the farther-from-shore AJ trajectory in neap tides (inset of Figure 8). As a result, particle concentration in Estepona is much higher in spring tide (Figure 8, solid lines). The deflection to the south of blue lines in the inset also illustrates the already discussed result of enhanced MPoP in Tetuan area in spring tides (Figure 6a). The progressive decrease of connectivity from HS to FS in spring-tide experiments (solid lines in left panel of Figure 8) follows the fact that eastward velocity reaches larger values during ebb tide (from HS to LS, peaking at ES) and a minimum at FS. Notice, however, that these differences are less than the ones observed between spring and neap tides (compare solid and dashed lines in this panel). It confirms the fact that tidal strength is more influential than tidal phase, what is further supported by the fortnightly modulation of ToMC in this area, with systematically shorter times in spring tides (Figure 6b).

The opposite situation is seen in Malaga area (Figure 8, right panel), where particle percentages in neap tides is almost twice than in spring tides. Moreover, as mentioned previously, ToMCs are greater in spring tides (Figure 6b). Inset in Figure 8 helps to explain these facts: during neap tides, a good fraction of trajectories invades directly the landing area (red lines), with reduced dispersion seaward. In spring tide, many particles arrive after having undergone some recirculation, a process that takes longer and results in greater ToMC, as discussed in Section 3.2.1. Also, more particles are scattered seaward, reducing the number of particles that reach the area. This behavior is shared by Roquetas and Carboneras landing areas to the east, confirming the better connectivity efficiency during neap tides (Figure 6).

3.4 | Depth dependence

Figure 6 and Figure 7 show that, on average, MPoP tends to increase with depth in all landing areas and for all releasing boxes and, simultaneously, ToMC tends to be shorter. On the other hand, the present uncertainty on the actual spawning depth of the blackspot seabream along with the marked baroclinity of the exchange through the SoG raises the question of whether the so far ignored westward connectivity gains prominence for hypothetical deeper layers of spawning. Both questions are addressed next

3.4.1 | A case study of south-to-north connectivity as function of depth

Figure 7a shows a rather clear increase of MPoP with depth in all landing areas of the north coast for particles released in Tangier-Med box. For Estepona area, this depth dependence is concomitant with the spring-neap fortnightly modulation. Overall, the influence of depth on the connectivity is less marked than that associated to tides and does not exhibit a regular pattern. Nevertheless, the diminution of the AJ intensity with depth allows for establishing a rough analogy between releasing depth and strength of the tide. For a given tidal condition, the patterns associated with releasing at the surface would differ from those at depth in a similar way to how patterns produced during spring tides differ from neap tides for a given depth.

Figure 9 illustrates the connectivity between Tangier-Med box and Estepona landing area under HN initial conditions (release at high water in neap tides). The larger surface current scatters more particles than the diminished current at 81 m depth, resembling the pattern observed in the case of spring against neap tides in the previous discussion. As a result, arrival time of particles released at surface levels ($z \leq 25$ m) in Tangier-Med box is noticeably shorter ($\sim$4 days) than that of particles released at 25 m (ToMC $\sim$7 days) or 81 m (ToMC $\sim$15 days), and the chance of arrival is notoriously reduced (MPoP of 17% for $z \leq 25$ m, which increases to 32% at 52 m and to 78% at 81 m, see also Figure 7a). As the depth increases, ELSs follow smoothed trajectories with reduced dispersion, which improves not
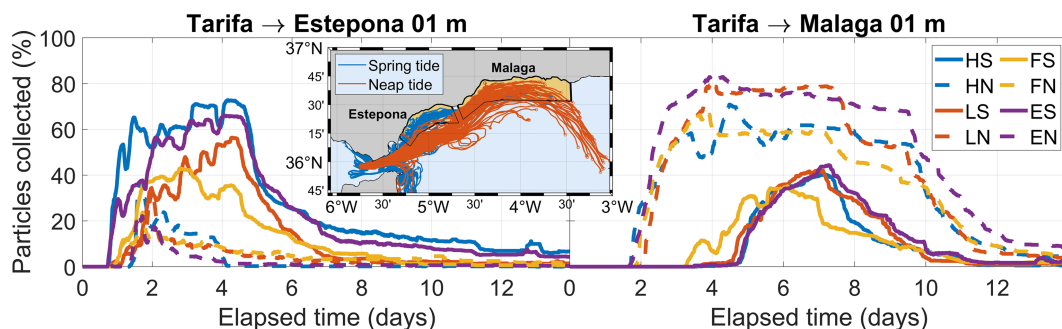

FIGURE 8 Time series of percentage of particles released at the surface in Tarifa releasing box collected in Estepona (left panel) and Malaga (right panel) for all tidal combinations discussed in text (see legend). The inset shows trajectories for the whole combination of phases in spring (blue lines) and neap (red lines) tides during the first 6 days after the release

FIGURE 9 Time series of percentage of particles released in Tangier-Med releasing box under HN conditions and collected in Estepona landing area for the five depths considered (1, 12, 25, 52, and 81 m). Inset map shows trajectories for surface and 81 m depth spawning levels after 30 days of simulation using the same color code as in the main panel
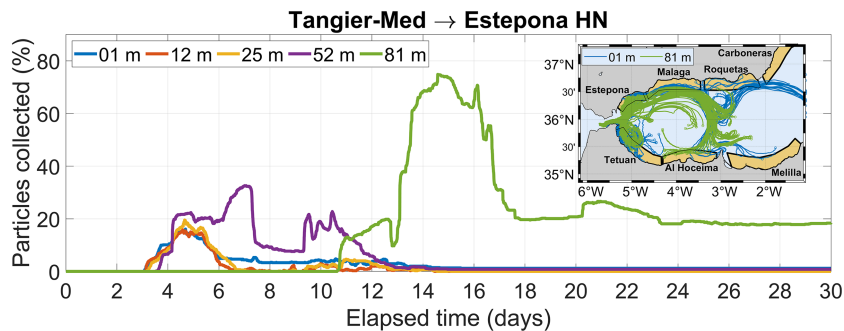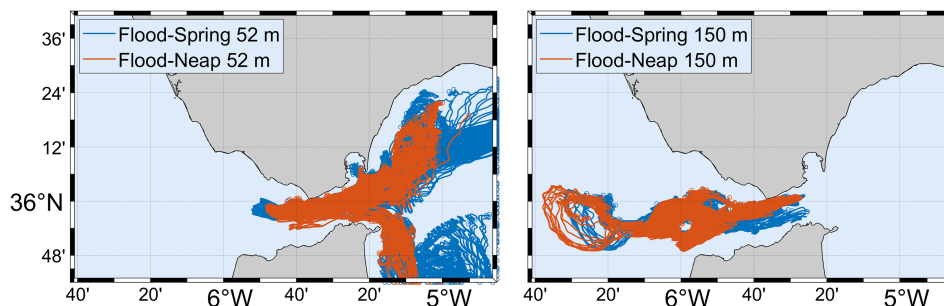

FIGURE 10 ELS trajectories after 3.5 days of simulation for particles released in Tarifa box at 52 m (left panel) and 150 m (right panel) in case of FS (blue lines) and FN (orange lines) initial conditions

only the chance for more particles to arrive but also for them to arrive further. The behavior, which can be applied to the other areas in the north coast, is similar to that described in neap tides for the connectivity Tarifa-Malaga.

3.4.2 | A sensitivity analysis on spawning depth in the SoG

The effect of depth on connectivity patterns, and its interaction with tide in the case of this species, raises the question of whether or not the species has adapted its life cycle to optimize the reproductive success. For instance, blackspot seabream should spawn at greater depths if the survival success relies on chances of reaching further landing areas (see previous section) with suitable nursery conditions. It represents a plausible method of colonization, which maximizes the population survival (Krueck et al., 2020). Selecting the highly dispersive environment of the SoG as spawning grounds almost rejects the hypothesis that this species attempts to maximize self-recruitment as observed in other species (e.g., European hake; Hidalgo et al., 2019). Since the SoG holds a permanent two-way exchange, depth results are critical to determine the direction of the ELS dispersion. At greater depths than those considered so far in the main study, eggs would be advected toward the Atlantic Ocean by the Mediterranean undercurrent and the connectivity with landing areas of the AS be drastically reduced.

Given the degree of uncertainty about the range of plausible spawning depths, it is worth exploring that possibility with the model. To this aim, a spawning depth of 150 m has been selected in Tarifa and Tangier-Med boxes and initial conditions of ES, EN, FS, and FN have been then applied.

Figure 10 shows the trajectories of particles released at 52 and 150 m under identical initial conditions of maximum westward tidal current at spring (FS) and neap (FN) tides. In the case of 52 m depth, particles make small incursions to the west transported by the flood, west-going tidal current that overcomes the average eastward inflow during short intervals. After this otherwise brief current reversal, particles enter the AS and remain there following trajectories similar to those depicted in the previous section. At the deeper layer of 150 m, however, flood tidal current increases the Mediterranean undercurrent extant at this depth and ELSs will spread westwards, with no particles entering the AS. Therefore, Atlantic (Cadiz and Arcila) landing areas are accessible as far as the direction of propagation is concerned. However, both landing areas are shallower than 100 m, whereas ELS propagates at 150 m. Unless vertical and onshore motions occur, the connectivity with the selected Atlantic landing areas is unfeasible.

The western half of the SoG is a well-known mixing area with large vertical motions driven by the amazing internal tide generated by topographic interaction (García-Lafuente et al., 2000, 2013; Wesson & Gregg, 1994). Such turbulent mixing is a potential mechanism to bring particles to shallower layers, in a similar manner as it does the westerly inducing upwelling and turbulence in the Gulf of Cadiz (Navarro et al., 2011; Sánchez Garrido et al., 2015). All of them can modify the horizontal depth of ELS advection but does not necessarily imply shoreward advection, which should be achieved by other concomitant processes. Recent scientific surveys have detected ELSs of the species in the Atlantic region, but their relative abundances are noticeably lower than those reported in the Alboran basin: 0.46 larvae 10 m^{-2} (±1.39 SD) in the Atlantic region *versus* 2.03 larvae 10 m^{-2} (4.86 SD) in the northwest Alboran areas (maximum abundances of 5 and 15 larvae 10 m^{-2}, respectively; J.M. Rodríguez, Pers. Comm.).

These observational and numerical results keep open the feasibility of the Atlantic connectivity, which requires further studies to give an adequate answer. Observational research on the spawning behavior is also needed to elucidate the question of the spawning depth range of the species. From a modeling perspective, new experiments are necessary to assess how different larval behavior (vertical migration) and hydrodynamic secondary patterns (vertical velocity ignored in this study) affect the dispersion patterns and survival probabilities of ELS under different scenarios.

3.5 | A sensitivity analysis on PLD

From a biological point of view, time of arrival of ELS at a given landing area only makes sense if it is less than the assumed PLD of the species (Shanks, 2009). In order to investigate the dependence of connectivity on PLD, MPoPs between releasing boxes and landing areas have been re-calculated for PLD windows of 15 and 30 days. The new values of MPoP (denoted by C_n, $n = 15, 30$, in the following discussion), have been compared with those of the original PLD window of 60 days (C_{60}) to obtain a metric Δ_n defined as the ratio:

$$\Delta_n = \frac{C_n}{C_{60}} \cdot 100$$

in order to assess the differences.

Table 3 summarizes the results of this analysis and confirms the fact that the MPoP is constrained by the available time of arrival, that is, the assumed PLD. In the landing areas nearest to the releasing boxes (i.e., Tangier-Med/Tangier – Tetuan, Tarifa – Estepona) arrival times keep on being short and maximum ratios obtained with different PLDs (15, 30, 60 days) are little altered (high values of Δ_n, $n = 15, 30$). On the contrary, in the furthest landing areas (Carboneras, Melilla, or Oran), large MPoPs are only obtained after completing a long path that requires dilated elapsed times, which makes the result sensitive to the assumed PLD. It results in substantial discrepancies (low ratio values). Extreme cases are provided by Tarifa-Carboneras or Tangier-Med/Tangier-Melilla, which shows ratios of Δ_{15} less than 1%.

The range of variation of the MPoPs recalls the need of improving the knowledge about the blackspot seabream life cycle, particularly PLD.

3.6 | Release time dependency (replicas)

To prove the representativeness and reliability of the Lagrangian particle tracking experiments, the uncertainty of each single run has been assessed by means of four replicas of the same combinations of semidiurnal tide and depth conditions during four fortnightly cycles. Despite the same initial conditions with respect to the releasing time, the overall situation is not exactly the same in the replicas. This is so because the four spring-neap tidal cycles considered comprises the monthly cycle arising from the modulation of the semidiurnal constituents M_2 and N_2, responsible for the greater similarity of alternate than contiguous spring cycles. In addition, subinertial meteorologically induced fluctuations due to atmospheric pressure and wind variations change from one replica to the other. The unavoidably, yet small, difference of the initial conditions of the replicas lead to concomitant differences in the outputs (not shown for the sake of clarity) and allows for assessing the variability of each experiment by means of the standard deviation of the four replicas. The averaged standard deviation of the whole pool of experiments is ~8%, which is approximately the same value obtained by comparing scenarios of different tidal phases but the same tidal strength. If the metric is used to compare spring and neap tidal scenarios (different tidal strength), the averaged standard deviation is ~30%. Therefore, subinertial variability and lower frequency tidal modulations could account for approximately one quarter of the variability of the fortnightly tidal cycle, which has been shown to be the prevailing factor for connectivity.

3.7 | Implications for the species assessment and management

Transboundary fish stock management is based in the cooperation and collaboration among countries to assess shared resources status and regulate harvest according to common measures and controls or

TABLE 3 Differences of MPoP computed using PLD windows of 60 and 30 days (Δ_{30} column) and 60 and 15 days (Δ_{15} column) for the three releasing boxes and the Alboran Sea landing areas

| | | MPoP differences (%) | | | | | |
| | | Tarifa | | Tangier-Med | | Tangier | |
Landing area		Δ_{15}	Δ_{30}	Δ_{15}	Δ_{30}	Δ_{15}	Δ_{30}
Northern Alboran	Estepona	77.69	92.79	49.65	83.79	50.22	84.40
	Malaga	62.02	94.37	62.49	94.20	63.20	95.60
	Roquetas	27.16	72.97	40.35	80.40	37.96	79.02
	Carboneras	0.92	36.55	2.290	31.31	1.610	26.19
Southern Alboran	Tetuan	89.90	95.92	96.10	98.60	95.56	99.16
	Al Hoceima	68.57	89.70	74.89	88.01	74.14	84.50
	Melilla	2.77	41.34	0.56	28.40	0.41	34.30
	Oran	7.44	55.11	3.59	61.64	1.47	60.07

Note: Cadiz and Arcila have been excluded because of its low representativeness.

joint decision-making. However, to build an effective management framework, a solid scientific basis is required. The present study provides this basis to potentially improve the assessment and management of this species harvested by Moroccan and Spanish fleets, while we acknowledge that further work is needed. First, it provides evidence of the differential role of different spawning grounds in the AS, which could be useful in the future if the spatial dynamics is implemented in the stock assessment models and procedures (e.g., Goethel & Berger, 2017; Punt, 2019). While the results of the study point at independent dispersal and connectivity patterns of north and south Strait spawning grounds due to the role of the AJ, they do not imply stock differentiation consistent with recent genetic studies (Spiga, 2020), but different spawning locations, which is an important element to be considered in spatial stock structure approaches. Second, in terms of spatial management and potential spatiotemporal closures already applied to other Mediterranean species (Regulation [EU] 2019/1022 of the European Parliament and of the Council of June 20, 2019, OJEU L172/1 and GFCM Recomm. GFCM/42/2018/5), the study facilitates information of the role of the spawning sites investigated, and also the interaction with depth and tidal regime that could potentially lead to seasonal or, even, short term (i.e., attending to tidal phase) fisheries closure. The information made available here is relevant for the ongoing process for the establishment of a specific joint (Spain and Morocco) management plan for blackspot seabream in the SoG within the framework of GFCM (2021). Notwithstanding, further studies are needed as it is not yet clear whether the spawning strategy of the species attempts to minimize dispersal time, maximize dispersal distance, or even a more complex trade-off between both. The interpretation and implications of the results presented in this study can be certainly different attending to the species strategy. The role of other important larval traits not included in this study requires also further research.

4 | SUMMARY AND FUTURE WORKS

The differences observed in the ELS connectivity patterns are mainly caused by the geographical location of the spawning areas in the SoG (north shore *versus* south shore). From a hydrodynamic perspective, the mean circulation patterns favor the zonal (west-to-east) connectivity: Particles released in the northern margin of the Strait are mostly registered in the northern areas of the AS, while particles released in the south are collected in the southern shores of the AS. Thus, the eastward transport linked to the AJ entering the Alboran basin appears as the main mechanism of connectivity. On the other hand, meridional connectivity (north-to-south, south-to-north) is hampered by the very AJ that is a potential hydrodynamic barrier (García-Lafuente, Sánchez-Garrido, et al., 2021). Overcoming this obstacle depends on the stability of the mean patterns of circulation of the SoG-AS system and its evolution. Non-geostrophic motions, instabilities associated with the WAG-AJ collapse (García-Lafuente et al., 1998; García-Lafuente, Sánchez-Garrido, et al., 2021; Sánchez-Garrido et al., 2013) or the AJ meandering (García-Lafuente &

Delgado, 2004) or, even, the WAG or EAG themselves can entail occasional meridional ELS transports. For instance, the study shows that ELSs released in Tangier-Med box are more susceptible to latitudinal (south-to-north) migration. Apparently, Tetuan area in the south exhibits characteristics of particle concentration/retention zone related to the existence of a small cyclonic eddy between the African coast and the WAG (Figure 1). Particle transfer from the eddy to the north-flowing western rim of gyre is practicable, after which particles reach the northern areas without impediment. This process impairs west-to-east connectivity in the south coast, which is therefore less efficient than in the north coast (compare Figures 6a and 7a). Another example is provided by the EAG, whose eastern edge can transport particles from the north to the south. This process makes Oran landing area be connected with Tarifa releasing box in the north better than with Tangier-Med in the south, despite being in the same coast (Table 2).

Atlantic, that is, east-to-west, connectivity at surface layers is prevented by the AJ. But it does not have to be so at greater depths where the Mediterranean undercurrent flows. In a hypothetical situation of deeper spawning (150 m), the model shows ELS transport towards the Atlantic Ocean exclusively, which opens the possibility of connection with landing areas in the Gulf of Cadiz (Cadiz, Arcila). However, achieving a successful connectivity with Atlantic landing areas requires additional processes to carry the ELS to shallower levels. Enhanced tidal mixing and turbulence occurring in the western part of the SoG, or wind-inducing upwelling in the Gulf of Cadiz are candidate processes.

Tides in the neighborhood of the SoG are influential. Variability due to tidal forcing is especially noticeable in terms of fortnightly modulation. In the landing areas closer to the spawning boxes (Estepona in the north, Tetuan in the south), connectivity is more efficient in spring tides. In these conditions, north-to-south connectivity is achieved by direct advection of ELSs from the releasing box of Tarifa to Tetuan landing area (Figure 6; see also inset in Figure 8). During neap tide, on the contrary, particles suffer less scattering and increase chances of reaching further landing areas. Overall, tidal conditions depict two different mechanisms: spring tides tend to favor connectivity (increase MPoP) by the direct advection promoted by the increased energy of the flows. It applies to landing areas adjacent to the releasing boxes in both, west-to-east and north-to-south, directions and yields relatively small ToMC. On the contrary, in neap tides connectivity is mainly achieved by the mean circulation of the AS, connecting far away landing areas with releasing boxes after considerably large ToMC (Figures 6 and 7). This pattern is consistent with previous studies on connectivity analysis in the region (Muñoz et al., 2015), who used altimetry-derived geostrophic currents, a product that removes tidal contribution during the data-processing. The circulation emerging from such an approach would be more similar to the pattern of neap tides (less tidal variability) inferred from the numerical outputs.

The depth of spawning also results in different patterns of conductivity. Obviously, the greatest differences arise when comparing patterns associated with spawning at depths immersed in one or

another layer of the baroclinic exchange, as illustrated by the case of 150 m releasing depth already discussed. But there are still differences even if spawning takes place at different depths within the very surface layer (Figures 6a and 7a). The origin of the differences has been ascribed to the diminution of the velocity of the current with depth. At shallow depths, ELSs are scattered more actively by the more energetic current, recalling the effect of the spring tide. At deeper layers, the main circulation weakens and allows ELS to move less chaotically and reach greater distances. The behavior resembles the pattern observed during neap tides, when far away areas are connected to the releasing boxes. Such connection may demand high ToMCs (Table 2, Figures 6b and 7b), which represent a potential constrain for connectivity, since the time must be less than PLD for obvious reasons. The need of improving the knowledge of blackspot seabream ontogeny, particularly the possible range of variation of its PLD, becomes crucial to achieve an optimization of the fishery management. As indicated in Faillettaz et al. (2018), this factor strongly influences the larval dispersal patterns and connectivity among adult subpopulations whose calculation is fully based in passive drifting larvae.

Larval dispersal studies rely on the dependence of numerous biological and physical key factors, which must be considered to determine broad-scale ecological connectivity. Egg buoyancy, vertical migrations, and the possible influences on the ELS fate of other biogeochemical features (Wor et al., 2017) are sensible information that is not yet well determined for the studied species (Gil, 2006), nor incorporated to the model. The 150 m depth case study addressed in this study illustrates how drastically different the results of connectivity can be. Even in the case that depths were restrict to the upper 100 m, the depth range mainly explored in this study (which results in connectivity patterns involving the AS exclusively), vertical motions in the SoG as well as other processes not considered, such as the egg buoyancy or the diel vertical cycle, can displace ELSs to greater depths. If so, part of the spawning products will go beyond the critical depth for which Atlantic connectivity is feasible. Covering these complexities is crucial to be able to implement fully 3D approaches, and, consequently, attain a more reliable vision of population dynamics of blackspot seabream and ultimately transfer this new knowledge to improve the management of this overexploited species. Further studies are needed as it is not yet clear whether the spawning strategy of the species attempts to minimize dispersal time, maximize dispersal distance, or even a more complex trade-off between both. The interpretation and implications of the results presented in this study can be certainly different attending to the species strategy. The role of other important larval traits not included in this study requires also further research that may help decision-makers to establish biological rest periods that lead to maximize connectivity and sustainability. All in all, improving our knowledge on the interaction of this species with its physical environment is a key issue in the efforts towards rebuilding the fishery target population until its maximum sustainable yield.

CONFLICT OF INTEREST

I hereby certify that there is no actual or potential conflict of interest in relation to this article.

AUTHOR CONTRIBUTION

IN, SS and JGL wrote the bulk of the paper. JGH contributed in the paper regarding the biological aspects of the blackspot seabream. MH and PH provided the fisheries arguments supporting the larvae dispersal patterns. IN, SS and JCSG designed and carried out the modeling experiments. All authors participated and contributed in the interpretation, discussion and revision of the manuscript.

AUTHOR DISCLAIMER

The views expressed in this publication are those of the author(s) and do not necessarily reflect the views or policies of the Food and Agriculture Organization of the United Nations.

DATA AVAILABILITY STATEMENT

The data that support the findings of this study are available from the corresponding author upon reasonable request.

ORCID

Irene Nadal https://orcid.org/0000-0002-1642-1606
Simone Sammartino https://orcid.org/0000-0001-7052-5468
Jesús García-Lafuente https://orcid.org/0000-0001-7816-576X
José C. Sánchez Garrido https://orcid.org/0000-0003-1524-7391
Juan Gil-Herrera https://orcid.org/0000-0001-8940-5749
Manuel Hidalgo https://orcid.org/0000-0002-3494-9658

REFERENCES

Albérola, C., Rousseau, S., Millot, C., Astraldi, M., Font, J., García-Lafuente, J., Gasparini, G. P., Send, U., & Vangriesheim, A. (1995). Tidal currents in the Western Mediterranean Sea. *Oceanologia Acta*, *18*(2), 273–284.

Alcaraz, J. L., Carrasco, J. F., Llera, E. M., Menéndez, M., Ortea, J. A., & Vizcaíno, A. (1987). *Aportación al estudio del besugo en el Principado de Asturias*. Recursos pesqueros de Asturias, 4. Servicio de publicaciones del Principado de Asturias.

Álvarez Fanjul, E., Pérez Gómez, B., & Sánchez-Arévalo, I. R. (2001). Nivmar: A storm surge forecasting system for Spanish Waters'. *65*(S1), 145–154. https://doi.org/10.3989/scimar.2001.65s1145

Báez, J. C., Macías, D., de Castro, M., Gómez-Gesteira, M., Gimeno, L., & Real, R. (2014). Assessing the response of exploited marine populations in a context of rapid climate change: The case of blackspot seabream from the Strait of Gibraltar. *Animal Biodiversity and Conservation*, *37*(1), 35–47. https://doi.org/10.32800/abc.2014.37.0035

Biagi, F., Gambaccini, S., & Zazzeta, M. (1998). Settlement and recruitment in fishes: The role of coastal areas. *The Italian Journal of Zoology*, *65*(Suppl), 269–274. https://doi.org/10.1080/11250009809386831

Brünnich, M. T. (1768). *Ichthyologia Massiliensis, sistens piscium descriptiones eorumque apud incolas nomina. Accedunt Spolia Maris Adriatici. Hafniae et Lipsiae*, i-xvi + 1-110, In 2 parts; first as i-xvi + 1-84; 2nd as Spolia e Mari Adriatica reportata: 85–110, 49.

Burgos, C., Gil, J., & del Olmo, L. A. (2013). The Spanish blackspot seabream (*Pagellus bogaraveo*) fishery in the Strait of Gibraltar: Spatial distribution and fishing effort derived from a small-scale GPRS/GSM based fisheries vessel monitoring system. *Aquatic Living Resources*, 26(4), 399–407. https://doi.org/10.1051/alr/2013068

CopeMed II. (2017). Report of the CopeMed II Workshop on methodologies for the identification of stock units in the Alboran Sea. Alicante, Spain, 3–6 April 2017. CopeMed II Technical documents N°46 (GCP/INT/028/SPA - GCP/INT/270/EC). Alicante, 58 pp.

CopeMed II. (2019). Report of the Mid-Term Workshop on TRANSBORAN project, "Transboundary population structure of sardine, European hake and blackspot seabream in the Alboran Sea and adjacent waters: a multidisciplinary approach" Malaga, Spain, 22–24 July 2019. CopeMed II Technical Documents N°52 (GCP/INT/028/SPA - GCP/INT/270/EC). Málaga, 33 pp.

Cowen, R. K., Paris, C. R., & Srinivasan, A. (2006). Scaling of connectivity in marine populations. *Science*, 311(5760), 522–527. https://doi.org/10.1126/science.1122039

Cowen, R. K., & Sponaugle, S. (2009). Larval dispersal and marine population connectivity. *Annual Review of Marine Science*, 1, 443–466. https://doi.org/10.1146/annurev.marine.010908.163757

Crochelet, E., Roberts, J., Lagabrielle, E., Obura, D., Petit, M., & Chabanet, P. (2016). A model-based assessment of reef larvae dispersal in the Western Indian Ocean reveals regional connectivity patterns—Potential implications for conservation policies. *Regional Studies in Marine Science*, 7, 159–167. https://doi.org/10.1016/j.rsma.2016.06.007

Desbrosses, P. (1932). La dorade commune (*Pagellus centrodontus*) et sa pêche. *Revue du Travail de L'Office Des Pêches Maritime*, 5, 167–222.

Dubois, M., Rossi, V., Ser-Giacomi, E., Arnaud-Haond, S., López, C., & Hernández-García, E. (2016). Large-scale connectivity and management of marine ecosystems. *Global Ecology and Biogeography*, 25, 503–515. https://doi.org/10.1111/geb.12431

Faillettaz, R., Paris, C., & Irisson, J.-O. (2018). Larval fish swimming behavior alters dispersal patterns from marine protected areas in the North-Western Mediterranean Sea. *Frontiers in Marine Science: Marine Ecosystem Ecology*, 5, 97. https://doi.org/10.3389/fmars.2018.00097

Fiksen, Ø., Jørgensen, C., Kristiansen, T., Vikebø, F., & Huse, G. (2007). Linking behavioural ecology and oceanography: Larval behaviour determines growth, mortality and dispersal. *Marine Ecology: Progress Series*, 347, 195–205. https://doi.org/10.3354/meps06978

Flexas, M. M., Gomis, D., Ruiz, S., Pascual, A., & León, P. (2006). In situ and satellite observations of the eastward migration of the Western Alboran Sea Gyre. *Progress in Oceanography*, 70, 486–509. https://doi.org/10.1016/j.pocean.2006.03.017

Fogarty, M., & Botsford, L. (2007). Population connectivity and spatial management of marine fisheries. *Oceanography*, 20(3), 112–123. https://doi.org/10.5670/oceanog.2007.34

Gamoyo, M., Obura, D., & Reason, C. (2019). Estimating connectivity through larval dispersal in the Western Indian Ocean. *Journal of Geophysical Research: Biogeosciences*, 124(8), 2446–2459. https://doi.org/10.1029/2019JG005128

García-Lafuente, J., Alvarez, E., Vargas, J. M., & Ratsimandresy, W. (2002). Subinertial variability in the flow through the strait of Gibraltar. *Journal of Geophysical Research*, 107(C10), 32.1–32.9. https://doi.org/10.1029/2001JC0011004

García-Lafuente, J., Bruque Pozas, E., Sánchez-Garrido, J. C., Sannino, G., & Sammartino, S. (2013). The interface mixing layer and the tidal dynamics at the eastern part of the Strait of Gibraltar. *Journal of Marine Systems*, 117–118, 31–42. https://doi.org/10.1016/j.jmarsys.2013.02.014

García-Lafuente, J., Cano, N., Vargas, M., Rubin, J. P., & Guerra, A. (1998). Evolution of the Alboran Sea hydrographic structures during July 1993. *Deep-Sea Research*, 45, 39–65. https://doi.org/10.1016/S0967-0637(97)00216-1

García-Lafuente, J., & Delgado, J. (2004). The meandering path of a drifter around the Western Alboran gyre. *Journal of Physical Oceanography*, 34(3), 685–692. https://doi.org/10.1175/3516.1

García-Lafuente, J., Sammartino, S., Huertas, I. E., Flecha, S., Sánchez-Leal, R., Naranjo, C., Nadal, I., & Bellanco, M. J. (2021). Hotter and weaker Mediterranean outflow as a response to basin-wide alterations. *Frontiers in Marine Science*, 8, 613444. https://doi.org/10.3389/fmars.2021.613444

García-Lafuente, J., Sánchez-Garrido, J. C., García, A., Hidalgo, M., Sammartino, S., & Laiz, R. (2021). Biophysical processes determining the connectivity of the Alboran Sea fish populations. In J. C. Báez, J. T. Vázquez, J. A. Caminas, & M. Malouli (Eds.), *Alboran Sea−Ecosystems and marine resources*. Springer Nature Switzerland AG. ISBN 978-3-030-65515-0. https://doi.org/10.1007/978-3-030-65516-7_12

García-Lafuente, J., Vargas, J. M., Plaza, F., Sarhan, T., Candela, J., & Bascheck, B. (2000). Tide at the eastern section of the Strait of Gibraltar. *Journal of Geophysical Research: Oceans*, 105(C6), 14197–14213. https://doi.org/10.1029/2000JC900007

GFCM. (2021). Report of the Working Group on Stock Assessment of Demersal species (WGSAD). General Fisheries Commission for the Mediterranean. Online, 18–30 January 2021.

Gil, J. (2006). Biología y pesca del voraz [*Pagellus bogaraveo* (Brünnich, 1768)] en el Estrecho de Gibraltar. PhD. Universidad de Cádiz.

Gil, J. (2010). Spanish information about the red seabream (*Pagellus bogaraveo*) fishery in the Strait of Gibraltar region. A CopeMed II contribution to the SRWG on shared demersal resources. Ad hoc scientific working group between Morocco and Spain on *Pagellus bogaraveo* in the Gibraltar Strait area (Málaga, Spain. 22 July, 2010). GCP/-INT/028/SPA-GCP/INT/006/EC. CopeMed II Occasional Paper N° 2: 30 pp.

Gil, J., Silva, L., & Sobrino, I. (2001). Results of two tagging surveys of red seabream [*Pagellus bogaraveo*, (Brünnich, 1768)] in the Spanish South Mediterranean region. *Thalassas*, 17(2), 43–46.

Gil-Herrera, J., Gutiérrez-Estrada, J. C., Benchoucha, S., Pérez-Gil, J. L., Sanz-Fernández, V., el Arraf, S., Burgos, C., Malouli Idrissi, M., & Farias, C. (2021). The Blackspot seabream fishery in the Strait of Gibraltar: Lessons and future perspectives of shared marine resource. In J. C. Báez, J. T. Vázquez, J. A. Caminas, & M. Malouli (Eds.), *Alboran Sea−Ecosystems and marine resources*. Springer Nature Switzerland AG. https://doi.org/10.1007/978-3-030-65516-7_19

Goethel, D. R., & Berger, A. M. (2017). Accounting for spatial complexities in the calculation of biological reference points: Effects of misdiagnosing population structure for stock status indicators. *Canadian Journal of Fisheries and Aquatic Sciences*, 74(11), 1878–1894. https://doi.org/10.1139/cjfas-2016-0290

Hidalgo, M., Rossi, V., Monroy, P., Ser-Giacomi, E., Hernández-García, E., Guijarro, B., Massutí, E., Alemany, F., Jadaud, A., Pérez, J. L., & Reglero, P. (2019). Accounting for ocean connectivity and hydroclimate in fish recruitment fluctuations within transboundary metapopulations. *Ecological Applications*, 29(5), e01913. https://doi.org/10.1002/eap.1913

Krueck, N., Treml, E., Innes, D., & Ovenden, J. (2020). Ocean currents and the population genetic signature of fish migrations. *Ecology (Ecological Society of America)*, 101(3), e02967. https://doi.org/10.1002/ecy.2967

Krug, H. M. (1994). Biologia e avaliaçao do stock Açoreano de goraz, *Pagellus bogaraveo*. PhD. Universidade dos Açores

LaCasce, J. H. (2008). Statistics from Lagrangian observations. *Progress in Oceanography*, 77, 1–29. https://doi.org/10.1016/j.pocean.2008.02.002

Lanoix, F. (1974) Projet Alboran, Etude hydrologique et dynamique de la Mer d'Alboran, Tech. lep. 66, 39 pp., NATO, Brussels.

Lorance, P. (2011). History and dynamics of the overexploitation of the blackspot sea bream (*Pagellus bogaraveo*) in the Bay of Biscay. *ICES Journal of Marine Science*, 68, 290–301. https://doi.org/10.1093/icesjms/fsq072

Marshall, J., Adcroft, A., Hill, C., Perelman, L., & Heisey, C. (1997). A finite-volume, incompressible Navier Stokes model for studies of the ocean on parallel computers. *Journal of Geophysical Research: Oceans*, 102(C3), 5753–5766. https://doi.org/10.1029/96JC02775

Marshall, J., Hill, C., Perelman, L., & Adcroft, A. (1997). Hydrostatic, quasi-hydrostatic and nonhydrostatic ocean modeling. *Journal of Geophysical Research: Oceans*, 102(C3), 5733–5752. https://doi.org/10.1029/96JC02776

Mason, E., Ruiz, S., Bourdalle-Badie, R., García-Sotillo, M., & Pascual, A. (2019). Copernicus (CMEMS) operational model intercomparison in the western Mediterranean Sea: Insights from an eddy tracker. *Ocean Science Discussions*, 15, 1111–1131. https://doi.org/10.5194/os-2018-169

Muñoz, M., Reul, A., Plaza, F., Gómez-Moreno, M. L., Vargas-Yáñez, M., Rodríguez, V., & Rodríguez, J. (2015). Implication of regionalization and connectivity analysis for marine spatial planning and coastal management in the Gulf of Cadiz and Alboran Sea. *Ocean and Coastal Management*, 118, 60–74. https://doi.org/10.1016/j.ocecoaman.2015.04.011

Navarro, G., Gutiérrez, F. J., Díez-Minguito, M., Losada, M. A., & Ruiz, J. (2011). Temporal and spatial variability in the Guadalquivir estuary: A challenge for real-time telemetry. *Ocean Dynamics*, 61, 753–765. https://doi.org/10.1007/s10236-011-0379-6

Nicolle, A., Dumas, F., Foveau, A., Foucher, E., & Thiébaut, E. (2013). Modelling larval dispersal of the king scallop (*Pecten maximus*) in the English Channel: Examples from the bay of Saint-Brieuc and the bay of Seine. *Ocean Dynamics*, 63, 661–678. https://doi.org/10.1007/s10236-013-0617-1

Nicolle, A., Moitié, R., Ogor, J., Dumas, F., Foveau, A., Foucher, E., & Thiébaut, E. (2017). Modelling larval dispersal of *Pecten maximus* in the English Channel: A tool for the spatial management of the stocks. *ICES Journal of Marine Science*, 74(6), 1812–1825. https://doi.org/10.1093/icesjms/fsw207

Olivier, R. (1928). Poissons de chalut. La dorade (*Pagellus centrodontus*) (Resume pratique de nos connaissances sur ce poisson). Rev. Trav. de l'Off. Peches Marit., Tome I, fasc. IV.

Palacios-Abrantes, J., Reygondeau, G., Wabnitz, C. C., & Cheung, W. W. (2020). The transboundary nature of the worlds exploited marine species. *Scientific Reports*, 10(1), 1–12. https://doi.org/10.1038/s41598-020-74644-2

Parrilla, G., & Kinder, T. H. (1987). The physical oceanography of the Alboran Sea, [Rep]. In *Meteorology and Oceanography*, 40 (Vol. 1) (pp. 143–184). Oceanogr. Group Div. of Applied Sciences, Harvard Univ.

Peleteiro, J. B., Olmedo, M., Gómez, C, & Álvarez-Blázquez, B. (1997). Study of reproduction in captivity of black-spot sea bream (*Pagellus bogaraveo*). Embryonic development and consumption of vitelline sac. ICES C.M. 1997/HH: 19

Pineda, J., Hare, J., & Sponaugle, S. (2007). Larval transport and dispersal in the coastal ocean and consequences for population connectivity. *Oceanography Society*, 20(3), 22–39. https://doi.org/10.5670/oceanog.2007.27

Pinho, M. R., Diogo, H., Carvalho, J., & Pereira, J. G. (2014). Harvesting juveniles of red (blackspot) seabream (*Pagellus bogaraveo B.*) in the Azores: Biologicalimplications, management and life cycle considerations. *ICES Journal of Marine Science*, 71(9), 2448–2456. https://doi.org/10.1093/icesjms/fsu089

Pinsky, M. L., Reygondeau, G., Caddell, R., Palacios-Abrantes, J., Spijkers, J., & Cheung, W. W. (2018). Preparing ocean governance for species on the move. *Science*, 360(6394), 1189–1191. https://doi.org/10.1126/science.aat2360

Punt, A. (2019). Spatial stock assessment methods: A viewpoint on current issues and assumptions. *Fisheries Research*, 213, 132–143. https://doi.org/10.1016/j.fishres.2019.01.014

Rodríguez, J. M., Barton, E. D., Eve, L., & Hernandez-Leon, S. (2001). Mesozooplankton and ichthyoplankton distribution around Gran Canaria, an oceanic island in the NE Atlantic. *Deep Sea Research, Part I*, 48(10), 2161–2183. https://doi.org/10.1016/S0967-0637(01)00013-9

Rossi, V., Ser-Giacomi, E., López, C., & Hernández-García, E. (2014). Hydrodynamic provinces and oceanic connectivity from a transport network help designing marine reserves. *Geophysical Research Letters*, 41(8), 2883–2891. https://doi.org/10.1002/2014GL059540

Ruti, P. M., Somot, S., Giorgi, F., Dubois, C., Flaounas, E., Obermann, A., DellAquila, A., Pisacane, G., Harzallah, A., Lombardi, E., Ahrens, B., Akhtar, N., Alias, A., Arsouze, T., Aznar, R., Bastin, S., Bartholy, J., Béranger, K., Beuvier, J., ... Vervatis, V. (2016). Med-CORDEX initiative for Mediterranean climate studies. *Bulletin of the American Meteorological Society*, 97(7), 1187–1208. https://doi.org/10.1175/BAMS-D-14-00176.1

Sakina-Dorothée, A., Pascal, L., & Éric, T. (2010). How does the connectivity between populations mediate range limits of marine invertebrates? A case study of larval dispersal between the Bay of Biscay and the English Channel (North-East Atlantic). *Progress in Oceanography*, 87(1–4), 18–36. https://doi.org/10.1016/j.pocean.2010.09.022

Sammartino, S., García-Lafuente, J., Naranjo, C., Sánchez-Garrido, J. C., Sánchez-Leal, R., & Sánchez-Román, A. (2015). Ten years of marine current measurements in Espartel Sill, Strait of Gibraltar. *Journal of Geophysical Research: Oceans*, 120, 6309–6328. https://doi.org/10.1002/2014JC010674

Sammartino, S., García-Lafuente, J., Sánchez Garrido, J. C., De los Santos, F. J., Álvarez Fanjul, E., Naranjo, C., Bruno, M., & Calero, C. (2014). Experimental and numerical characterization of harbor oscillations in the port of Málaga, Spain. *Continental Shelf Research*, 72, 34–36. https://doi.org/10.1016/j.oceaneng.2014.06.011

Sammartino, S., Sánchez-Garrido, J. C., Naranjo, C., García-Lafuente, J., Rodríguez-Rubio, P., & Sotillo, M. (2018). Water renewal in semi-enclosed basins: A high resolution Lagrangian approach with application to the Bay of Algeciras, Strait of Gibraltar. *Limnology and Oceanography: Methods*, 16, 106–118. https://doi.org/10.1002/lom3.10231

Sánchez, F. (1983). Biology and fishery of the red sea-bream (*Pagellus bogaraveo B.*) in VI, VII and VIII Subareas of ICES. ICES C.M. 1983/G:38.

Sánchez Garrido, J. C., Naranjo, C., Macías, D., García-Lafuente, J., & Oguz, T. (2015). Modeling the impact of tidal flows on the biological productivity of the Alboran Sea. *Journal of Geophysical Research: Oceans*, 120(11), 7329–7345. https://doi.org/10.1002/2015JC010885

Sánchez-Garrido, J. C., García-Lafuente, J., Álvarez Fanjul, E., García Sotillo, M., & de los Santos, F. J. (2013). What does cause the collapse of the Western Alboran Gyre? Results of an operational ocean model. *Progress in Oceanography*, 116, 142–153. https://doi.org/10.1016/j.pocean.2013.07.002

Sánchez-Garrido, J. C., Sannino, G., Liberti, L., García-Lafuente, J., & Pratt, L. (2011). Numerical modeling of three-dimensional stratified tidal flow over Camarinal Sill, Strait of Gibraltar. *Journal of Geophysical Research*, 116, C12026. https://doi.org/10.1029/2011JC007093

Sarhan, T., García-Lafuente, J., Vargas, M., Vargas, J. M., & Plaza, F. (2000). Upwelling mechanisms in the northwestern Alboran Sea. *Journal of Marine Systems*, 23(4), 317–331. https://doi.org/10.1016/S0924-7963(99)00068-8

Shanks, A. L. (2009). Pelagic larval duration and dispersal distance revisited. *The Biological Bulletin*, 216(3), 373–385. https://doi.org/10.1086/BBLv216n3p373

Sotillo, M. G., Cailleau, S., Lorente, P., Levier, B., Aznar, R., Reffray, G., Amo-Baladrón, A., Chanut, J., Benkiran, M., & Alvarez-Fanjul, E. (2015). The MyOcean IBI ocean forecast and reanalysis systems: Operational products and roadmap to the future Copernicus service. *Journal of Operational Oceanography*, *8*(1), 63–79. https://doi.org/10.1080/1755876X.2015.1014663

Spiga, M. (2020). A multidisciplinar approach to assess population structure of *Pagellus bogaraveo* for a correct delineation of stock units in the Alboran Sea. University of Bologna. MSc Thesis. 74 pp.

Sundby, S., & Kristiansen, T. (2015). The principles of buoyancy in marine fish eggs and their vertical distributions across the World Oceans. *PLoS ONE*, *10*(10), e0138821. https://doi.org/10.1371/journal.pone.0138821

Sundelöf, A., & Jonsson, P. R. (2012). Larval dispersal and vertical migration behaviour—A simulation study for short dispersal times. *Marine Ecology*, *33*, 183–193. https://doi.org/10.1111/j.1439-0485.2011.00485

Taylor, G. I. (1922). Diffusion continuous movements. *Proceedings of the London Mathematical Society*, *20*, 196–212. https://doi.org/10.1112/plms/s2-20.1.196

Vargas-Yáñez, M., Plaza, F., García-Lafuente, J., Sarhan, T., Vargas, J. M., & Vélez-Belchi, P. (2002). About the seasonal variability of the Alboran Sea circulation. *Journal of Marine Systems*, *35*(3–4), 229–248. https://doi.org/10.1016/S0924-7963(02)00128-8

Virtanen, E. A., Moilanen, A., & Viitasalo, M. (2020). Marine connectivity in spatial conservation planning: Analogues from the terrestrial realm. *Landscape Ecology*, *35*(5), 1021–1034. https://doi.org/10.1007/s10980-020-00997-8

Wesson, J. C., & Gregg, M. C. (1994). Mixing at Camarinal Sill in the Strait of Gibraltar. *Journal of Geophysical Research: Oceans*, *99*(C5), 9847–9878. https://doi.org/10.1029/94JC00256

Wor, C., McAllister, M., Martell, S., & Taylor, N. (2017). A Lagrangian approach to model movement of migratory species. *Canadian Journal of Fisheries and Aquatic Sciences*, *75*(8), 1203–1214. https://doi.org/10.1139/cjfas-2017-0093

SUPPORTING INFORMATION

Additional supporting information may be found in the online version of the article at the publisher's website.